Binbin Lu,[1] Dave Bridges,[1] Yemen Yang,[1] Kaleigh Fisher,[1] Alan Cheng,[1] Louise Chang,[1] Zhuo-Xian Meng,[1] Jiandie D. Lin,[1] Michael Downes,[2] Ruth T. Yu,[2] Christopher Liddle,[2,3] Ronald M. Evans,[2] and Alan R. Saltiel[1]

Metabolic Crosstalk: Molecular Links Between Glycogen and Lipid Metabolism in Obesity

Diabetes 2014;63:2935–2948 | DOI: 10.2337/db13-1531

Glycogen and lipids are major storage forms of energy that are tightly regulated by hormones and metabolic signals. We demonstrate that feeding mice a high-fat diet (HFD) increases hepatic glycogen due to increased expression of the glycogenic scaffolding protein PTG/R5. PTG promoter activity was increased and glycogen levels were augmented in mice and cells after activation of the mechanistic target of rapamycin complex 1 (mTORC1) and its downstream target SREBP1. Deletion of the PTG gene in mice prevented HFD-induced hepatic glycogen accumulation. Of note, PTG deletion also blocked hepatic steatosis in HFD-fed mice and reduced the expression of numerous lipogenic genes. Additionally, PTG deletion reduced fasting glucose and insulin levels in obese mice while improving insulin sensitivity, a result of reduced hepatic glucose output. This metabolic crosstalk was due to decreased mTORC1 and SREBP activity in PTG knockout mice or knockdown cells, suggesting a positive feedback loop in which once accumulated, glycogen stimulates the mTORC1/SREBP1 pathway to shift energy storage to lipogenesis. Together, these data reveal a previously unappreciated broad role for glycogen in the control of energy homeostasis.

Glycogen represents the first choice for energy storage and use. Its metabolism is tightly regulated by both hormones and nutritional status, which control the activities of glycogen synthase (GS) and glycogen phosphorylase (GP) through a variety of pathways (1). GS and GP activities are coordinated by glycogen-targeting subunits that serve as molecular scaffolds, bringing together these enzymes with phosphatases and kinases in a macromolecular complex and in the process, promoting activation of GS and inactivation of GP. Six different proteins target protein phosphatase 1 (PP1) to glycogen (2). In liver, PTG and GL are expressed at approximately equivalent levels (3), and together, they facilitate the mobilization and storage of hepatic glycogen. PTG overexpression dramatically increases glycogen content because of a redistribution of PP1 and GS to glycogen particles and a corresponding marked increase in GS activity and glycogen synthesis (4–8).

Despite its profound effects, how PTG controls glycogen metabolism remains uncertain. One potential mode of regulation may be transcriptional. Both noradrenaline and adenosine upregulate PTG mRNA levels in astrocytes and hepatocytes concomitant with increased glycogen synthesis (9). The FoxA2 forkhead class transcription factor directly binds to and transactivates the PTG promoter in vitro (10). Moreover, two SREBP/upstream stimulatory factor–binding units in the PTG promoter also suggest potential transcriptional regulation by SREBP.

These indications that PTG may be under transcriptional regulation prompted us to study its expression during various dietary conditions and assess its importance in energy homeostasis. We show that a high-fat diet (HFD) produces an increase in hepatic glycogen through a process that involves induction of PTG mRNA and protein levels, which occur downstream of mechanistic

[1]Life Sciences Institute, University of Michigan, Ann Arbor, MI
[2]Salk Institute for Biological Sciences, La Jolla, CA
[3]Storr Liver Unit, Westmead Millennium Institute and University of Sydney, Westmead Hospital, Westmead, NSW, Australia

Corresponding author: Alan R. Saltiel, saltiel@umich.edu.

Received 4 October 2013 and accepted 2 April 2014.

This article contains Supplementary Data online at http://diabetes.diabetesjournals.org/lookup/suppl/doi:10.2337/db13-1531/-/DC1.

D.B. is currently affiliated with the Department of Physiology, University of Tennessee Health Science Center, Memphis, TN, and the Children's Foundation Research Institute, Le Bonheur Children's Hospital, Department of Pediatrics, University of Tennessee Health Science Center, Memphis, TN.

A.C. is currently affiliated with the Department of Biochemistry and Molecular Biology, University of Louisville School of Medicine, Louisville, KY.

target of rapamycin complex 1 (mTORC1) activation and SREBP1 induction. Of note, PTG knockout (KO) mice fed an HFD exhibited not only decreased glycogen levels in liver but also improved insulin sensitivity as well as decreased hepatic steatosis, both of which can be attributed to reduced activation of mTORC1. Taken together, these data indicate that upon its accumulation in the liver, glycogen elicits a positive feedback loop involving mTORC1, resulting in increased expression of lipogenic genes and, thus, a coordinated synthesis of glycogen and lipids.

RESEARCH DESIGN AND METHODS

Animals

Generation of PTG KO mice has been described previously (11). These mice had been maintained on a mixed genetic background, but for these studies, they were crossed 10 times with C57BL/6J mice (The Jackson Laboratory). Wild-type (WT) littermates were used as controls. At 8–10 weeks, male mice were either fed an HFD containing 45% fat (D12451; Research Diets Inc.) or continued on a normal diet (ND) containing 4.5% fat (5L0D; LabDiet) for the same duration. All mice were maintained in temperature- and humidity-controlled conditions with a 12-h light/dark cycle and free access to food and water. All protocols were approved by the University of Michigan Animal Care and Use Committee.

Antibodies

The following antibodies were used: GS, pGS (S641), S6K1, pS6K1 (T389), S6, and pS6 (S235/236) (all from Cell Signaling) and SREBP1 (a gift from J. Horton). PTG was detected after amylose pull-down (AMPD) assay using a rabbit polyclonal antibody raised against the murine PTG sequence as described previously (11). A mouse monoclonal antibody raised against RalA (BD Biosciences) and rabbit polyclonal antibody raised against CREB (Cell Signaling) were used as a loading control for whole-cell lysate and nuclear extracts, respectively. For detection, a Western Lightning Plus-ECL Enhanced Chemiluminescence Substrate kit (PerkinElmer Life Sciences) was used. Individual protein bands were quantified by NIH ImageJ software.

Glycogen Measurement and Assay of Glucose Conversion Into Glycogen

Glycogen was measured as previously published (12). The assay of glucose conversion into glycogen was performed as previously described (13).

Triglyceride Measurement

Frozen tissues were homogenized in buffer containing 50 mmol/L Tris, 5 mmol/L EDTA, and 30 mmol/L mannitol. Crude lysate was mixed with potassium hydroxide and extracted with chloroform:methanol (2:1). After vigorous vortexing and short incubation, samples were centrifuged at 13,000 rpm for 10 min. The bottom layer was dried and resuspended in butanol mixture (3 mL butanol, 1.66 mL Triton X-114, and 0.33 mL methanol) before assaying the triglyceride content with a Serum Triglyceride Determination Kit (Sigma-Aldrich).

Quantitative Real-Time PCR

Total RNA was isolated (Ambion RNA isolation kit; Life Technologies) and subjected to quantitative real-time PCR as described previously (14). Primers are listed in Supplementary Table 1.

Western Blotting and AMPD Assay

Whole-cell lysates and nuclear extracts were prepared as described previously (11,15). AMPD assays were used to analyze PTG and glycogen-bound GS protein levels. Briefly, 1 mg total proteins from crude lysates was incubated with amylose resin (New England Biolabs) for 2 h at 4°C before centrifuged down at 3,000 rpm for 2 min. Proteins bound to the resin were washed and released by boiling in the presence of SDS sample buffer and subjected to Western blotting.

Luciferase Constructs and Luciferase Reporter Assay

PTG promoter fragments were generated as described previously (10). The −493 to +36 fragment was used as a template to produce mutations in the putative SREBP binding sites. The following primer sequences were used in site-directed mutagenesis: M1, 5′-GATTGGTCGGAGGGACCGT GGCTTTGATAAGCTGCC-3′ and 5′-GGCAGCTTATCAAAGC CACGGTCCCTCCGACCAATC-3′; M2, 5′ GATTGGTCGGAGG GACCGGTTGTCGTGATCTGGCTTTGATAAG-3′and 5′- CT TATCAAAGCCAGATCACGACAACCGGTCCCTCCGACCAAT C-3′; and M3, 5′- GTCGGAGGGACCGGTTGTCGACATCTG GCTTTGATAAGCTGC-3′ and 5′-GCAGCTTATCAAAGCCA GATGTCGACAACCGGTCCCTCCGAC-3′. Human embryonic kidney (HEK) 293A and TSC2 murine embryonic fibroblast (MEF) cells were cultured in DMEM containing 10% FBS. TSC2-null MEFs were obtained from D. Kwiatkowski (Brigham and Women's Hospital) (16). Luciferase reporter assay was conducted as described previously (10).

Chromatin Immunoprecipitation Assay

TSC2 MEF cells were treated with 1% formaldehyde for 10 min and processed with a chromatin immunoprecipitation (ChIP) assay kit as described previously (10). An aliquot of DNA was used for quantitative real-time PCR using the following primers corresponding to the mouse PTG genomic sequences: P1, 5′-CTGGAGTTCCAGGCTGTGTA-3′ and 5′-GAGAACGGCTCAGAGGGTAG-3′; P2, 5′-GGGAAACACACA CACACACA-3′ and 5′-GAGAAGTTGGCTGGCTCTTC-3′; P3, 5′-TCACGTGATCTGGCTTTGAT-3′ and 5′-CTGAGCAACTTC GCACTCAG-3′; and P4, 5′-TTTGATTGGTCGGAGGGA-3′ and 5′-AACCGGGAGGCAGCTTAT-3′.

Blood Glucose and Insulin Measurements

Blood glucose was measured by a OneTouch Ultra glucometer (LifeScan). Plasma insulin concentrations were measured by Ultra Sensitive Mouse Insulin ELISA Kit (Crystal Chem, Inc.).

Glucose, Insulin, and Pyruvate Tolerance Tests

For glucose tolerance tests (GTTs), mice were fasted for 6 h before an oral injection of glucose (1.5 g/kg body weight). For insulin tolerance tests (ITTs), mice were fasted for 3 h before an injection of Humulin R (Eli Lilly) (0.75 units/kg

body weight i.p. for ND or 1.5 units/kg body weight i.p. for HFD). For pyruvate tolerance tests (PTTs), mice were fasted overnight before an injection of sodium pyruvate (1.5 g/kg body weight i.p.). Blood glucose concentrations were measured before and after the injection at the indicated time points using the OneTouch Ultra glucometer.

Short Hairpin RNA Knockdown Experiments

Mouse pGIPZ lentiviral–short hairpin RNA (shRNA) clones targeting SREBP1 and PTG were provided by the University of Michigan Biomedical Research Core Facilities. Lentiviral production was done as described previously (17).

RNA Sequencing and Data Analysis

Total RNA was isolated from livers of biological triplicates using TRIzol (Invitrogen) and the RNeasy Mini Kit (Qiagen). Libraries were prepared from 100–500 ng total RNA (TrueSeq Sample Preparation Kit v2; Illumina) and sequenced on the Illumina HiSeq 2000 using bar-coded multiplexing and a 100-bp read length. Data analysis was accomplished as previously described (16) using UCSC mm9 as a reference sequence. Heat maps were visualized using Java TreeView 1.1.6r2 (http://jtreeview.sourceforge.net). RNA sequencing (RNA-seq) data are available from the Gene Expression Omnibus (www.ncbi.nlm.nih.gov/geo) as accession no. GSE45319.

RESULTS

HFD Increases Hepatic Glycogen in Fasted Mice

To understand better the role of glycogen metabolism in the overall control of energy disposition, C57BL/6J mice were fed an HFD for 12 weeks and became obese, glucose intolerant, and insulin resistant (Supplementary Fig. 1). Mice were subjected to 16 h of fasting followed by 6 h of refeeding before kill. Hepatic glycogen levels were almost completely depleted by fasting and replenished after refeeding (Fig. 1*A*). Of note, although levels were similar in the refed state, HFD produced a threefold increase in hepatic glycogen levels in fasted mice (Fig. 1*A*). Hepatic PTG (*Ppp1r3c*) mRNA levels were increased approximately twofold by HFD in both the fasted and the refed states, concomitant with similar induction in SREBP1 (*Srebf1*) mRNA levels (Fig. 1*B*). Phosphorylation of the mTORC1 downstream target S6K and its substrate S6 was dramatically increased by HFD in fasted mice (Fig. 1*C*). Fasting reduced SREBP1 processing; however, we still detected an increase in the active, mature form of SREBP1 protein after HFD (Fig. 1*C*), which is consistent with previous reports (17,18). PTG protein levels corresponded well with the HFD-dependent increase in mTORC1 activity and SREBP1 induction (Fig. 1*C*), suggesting that the mTORC1/SREBP1 pathway contributes to the elevated glycogenesis observed in obesity in the fasted state.

GP activity did not change, ruling out the possibility that increased glycogen content in obesity results from reduced GP activity (Fig. 1*D*). Although total GS protein levels decreased during refeeding, the mRNA levels of the predominant GS isoform *GYS2* in liver were not changed, suggesting a posttranscriptional modification of GS in response to refeeding (Fig. 1*B*). Because the GS antibody might not efficiently recognize the dephosphorylated form of the enzyme, we measured GS activity (−/+G6P ratio) in liver lysate and observed increased GS activity in response to refeeding in the livers of ND-fed but not HFD-fed mice (Fig. 1*E*).

The PTG Promoter Is Regulated by SREBP1 and mTORC1

The coordinated increases in hepatic SREBP1 and PTG protein and transcript levels in response to nutritional status and the correlation of these findings with increased glycogen levels suggested an SREBP-dependent mechanism for the regulation of PTG transcription. Therefore, we generated mutations of SREBP binding sites on the PTG promoter (10) and assessed their activities by luciferase-based promoter assays. Expression of active SREBP-1c led to an approximately twofold increase in the activity of the WT PTG promoter, an effect significantly blunted in the mutants (Fig. 2*A*), suggesting that SREBP1 modulates PTG promoter activity through sterol regulatory elements (SREs) proximal to the transcriptional start site.

To determine whether mTORC1 can regulate PTG transcript levels, we examined $TSC2^{-/-}$ MEFs that have high mTORC1 activity (19). PTG promoter activity was elevated in $TSC2^{-/-}$ cells and was reduced by rapamycin treatment (Fig. 2*B*). However, this activation was not seen in the PTG promoter mutant M1, in which the only available SRE was deleted. ChIP assay confirmed direct interaction of SREBP1 with the PTG promoter, and this interaction was enhanced at the SREBP1 binding site by constitutive activation of mTORC1 (Fig. 2*C*). Similarly, overexpression of the constitutively active form of Rheb (20) activated the PTG promoter in a rapamycin-sensitive manner, and this effect was abolished by deletion of the proximal SRE in the PTG promoter (Fig. 2*D*).

Transcriptional Regulation of PTG Expression by SREBP1 Is Required for the Increased Glycogen Produced by mTORC1 Activation

$TSC2^{-/-}$ MEFs have increased protein levels of PTG and SREBP1, higher steady state levels of glycogen, and a greater rate of glucose conversion into glycogen than WT MEFs (Fig. 3*A*, *C*, and *D* [control]), suggesting that mTORC1 activation is sufficient for increased glycogen content in vitro. Because PTG binds to and localizes PP1 and its substrate GS to glycogen (4), we performed AMPD assays to measure PTG and GS bound to a glycogen-like matrix. Glycogen-bound GS levels increased with PTG (Fig. 3*A*, control), explaining the elevated glycogen content in $TSC2^{-/-}$ cells. These data reinforce the notion that PTG plays a dual scaffolding/dephosphorylation role by recruiting GS to the glycogen pellet and promoting its dephosphorylation.

To test whether the stimulation of glycogen synthesis by mTORC1 depends on SREBP1, we performed lentiviral-mediated shRNA knockdown of SREBP1. The levels of PTG protein and mRNA were reduced by SREBP1

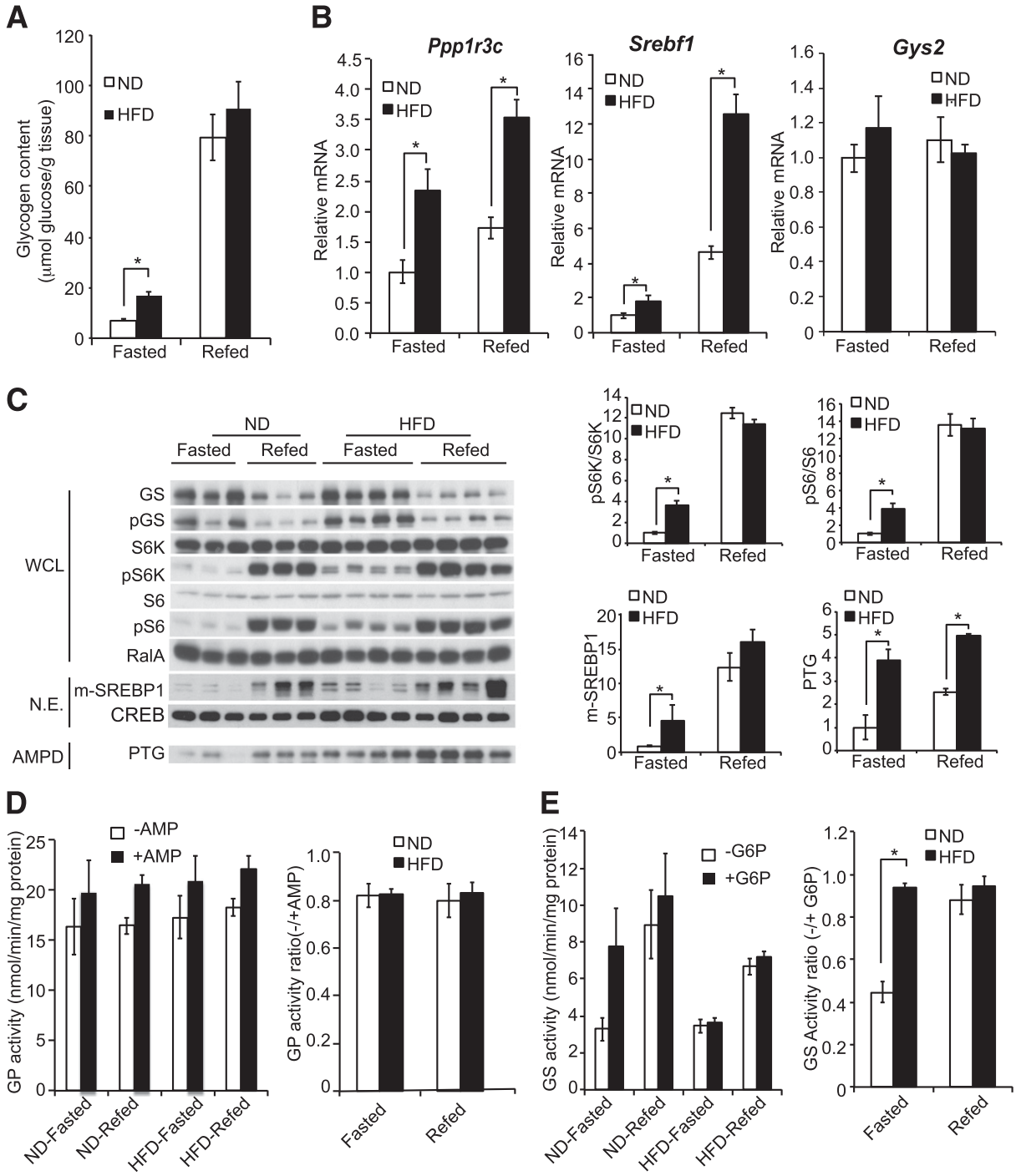

Figure 1—HFD increases hepatic glycogen in fasted mice. *A*: Glycogen content in the liver of C57BL/6J mice fed HFD for 12 weeks and killed after 16 h of fasting followed by 6 h of refeeding (n = 8 each group). *B*: Quantitative real-time PCR showing relative mRNA level of PTG, SREBP1, and GYS2 from the liver of mice in *A*. *C*: Representative Western blots from the liver of mice in *A*. See RESEARCH DESIGN AND METHODS for details. N.E., nuclear extracts; WCL, whole-cell lysate. *D* and *E*: Hepatic GP and GS activity, respectively, from the mice in *A* (n = 6–8 mice/group). Data are mean ± SE. *P < 0.05 by Student t test.

knockdown, as was the recruitment of GS to the amylose precipitate (Fig. 3*A* and *B*). Glycogen levels (Fig. 3*C*) and the conversion of glucose into glycogen (Fig. 3*D*) were similarly reduced. Collectively, these data suggest a role for mTORC1 in the regulation of PTG gene expression through SREBP binding to an SRE in the PTG promoter.

PTG Levels Control Glycogen Synthesis and Contribute to Feedback Regulation of mTORC1 and SREBP1

Lentiviral-mediated shRNA knockdown of PTG produced a 60–70% reduction in both protein and transcript levels of PTG in TSC2$^{-/-}$ cells (Fig. 4*A* and *B*). PTG knockdown

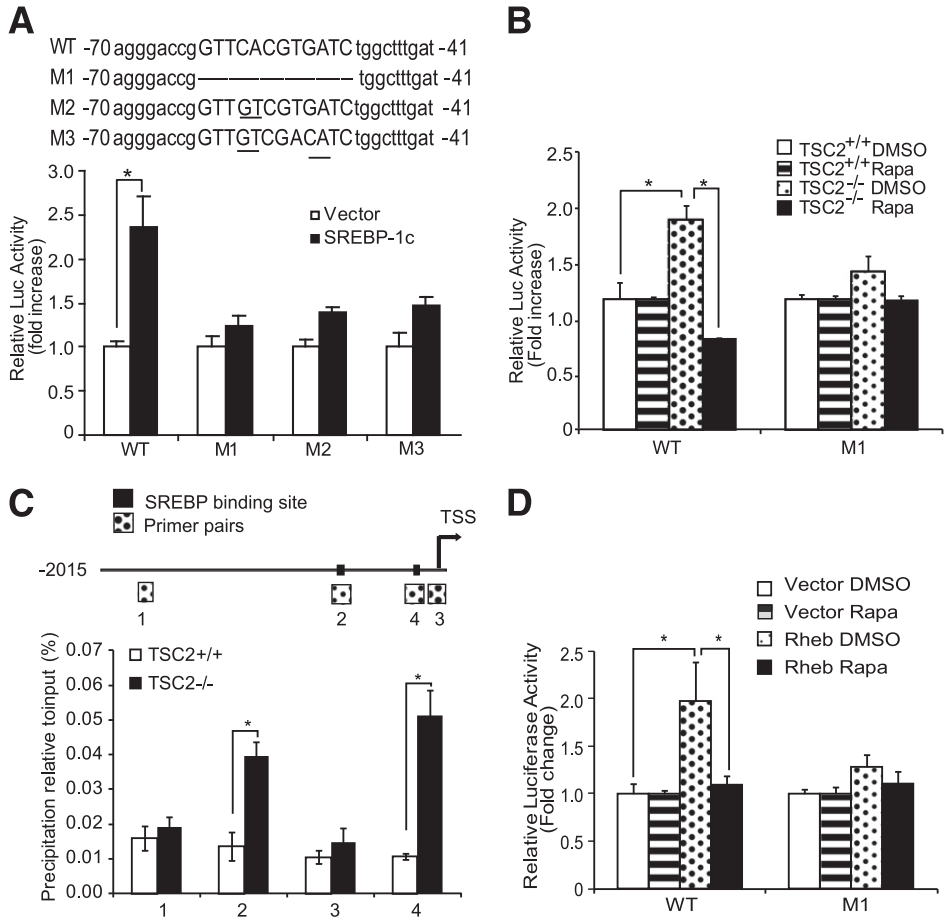

Figure 2—The PTG promoter is regulated by SREBP1 and mTORC1. *A*: HEK293 cells were cotransfected with a nuclear active form of SREBP-1c (aa 1–471) and the indicated reporter constructs of the PTG promoter. Cells were harvested 24 h after transfection and assayed for luciferase activity. Results were normalized (Renilla luciferase) and expressed as fold increase over the basal value of each construct. *B*: TSC2 MEF cells were transfected with the indicated luciferase reporter constructs of the PTG promoter and treated with rapamycin (100 nmol/L) or DMSO before harvest. *C*: A schematic representation of the PTG promoter region (*top*) and ChIP experiment showing increased SREBP1 activity in TSC2$^{-/-}$ cells (*bottom*). Cross-linked chromatin was immunoprecipitated with SREBP1 antibody and extensively washed before elution and precipitation of DNA. Quantitative PCR was performed with the indicated primer pairs. Primer sequences are listed in RESEARCH DESIGN AND METHODS. *D*: Effect of Rheb and rapamycin on the PTG promoter activity. HEK293 cells were cotransfected with Rheb or vector and the indicated luciferase reporter construct of the PTG promoter harboring the deletion of the putative SREBP1 binding site. Cells were subsequently treated with DMSO or rapamycin (100 nmol/L) for 24 h before harvest and assayed for luciferase activity. Results were normalized (Renilla luciferase) and expressed as fold increase over the basal value of each construct. Data are mean ± SE (n = 3). *P < 0.05 by Student t test. Luc, luciferase; Rapa, rapamycin; TSS, transcription start site.

did not affect other glycogen-targeting subunits, such as GL, GM, and the catalytic subunit PP1 (Supplementary Fig. 2*A* and *B* and Fig. 4*A*). Of note, PTG knockdown also reduced SREBP1 protein and mRNA levels, suggesting a positive feedback mechanism in which PTG regulates SREBP1.

PTG knockdown produced a 60–70% reduction in both steady state glycogen content and rate of glycogen synthesis in TSC$^{-/-}$ but not TSC$^{+/+}$ cells (Fig. 4*C* and *D*), consistent with the knockdown efficiency of PTG in these cells. The reduced glycogen synthesis was not due to reduced glucose transport because glucose uptake was not affected by PTG knockdown (Fig. 4*E*).

We next examined regulation of mTORC1 activity and glycogen levels by PTG in HEK293A cells in which we stably overexpressed Flag-GFP–tagged PTG. Glycogen levels in these cells were 50-fold higher than in control cells (Fig. 4*F*) because of the constitutive activation of PTG proteins (Fig. 4*G*). Moreover, phosphorylation of S6K was increased twofold in cells overexpressing PTG (Fig. 4*G*), suggesting that the scaffolding protein also regulates mTORC1 signaling through a positive feedback mechanism. Taken together, these results provide evidence that regulation of PTG expression is directly responsible for the increased glycogen levels in the context of activated mTORC1.

In HEK293A cells and the liver cell line Hepa1c, we also observed similar regulation of glycogen synthesis through PTG. Transient overexpression of WT PTG in these cells resulted in a two- to threefold increase in glycogen

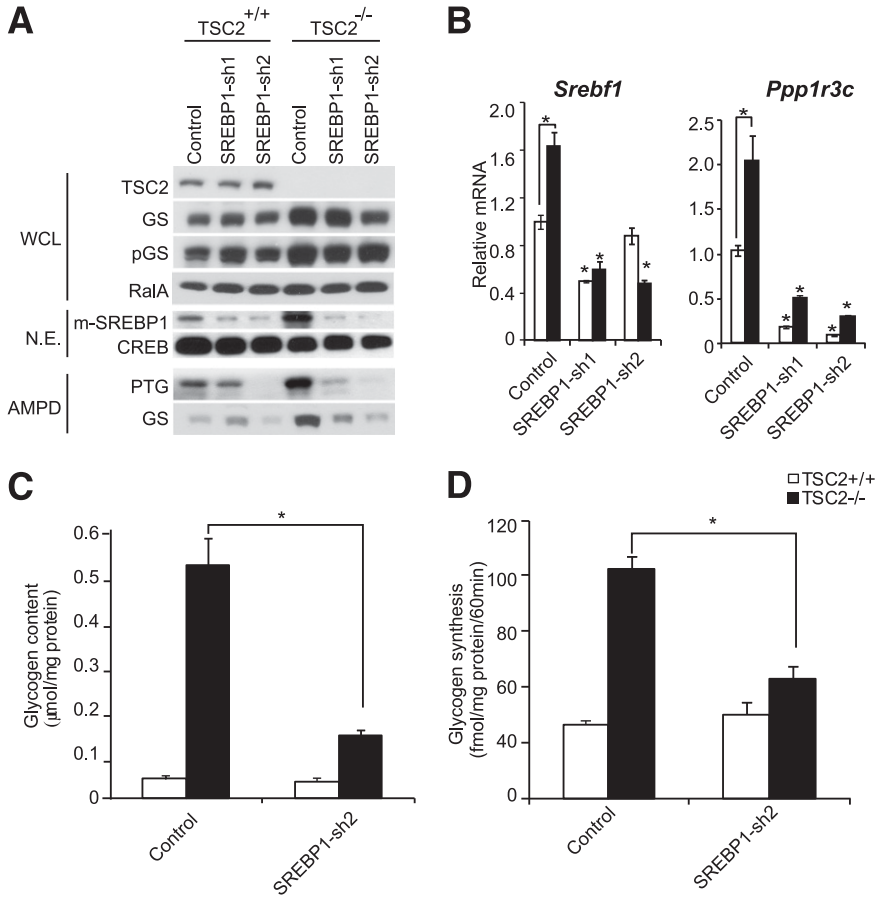

Figure 3—Transcriptional regulation of PTG expression by SREBP1 is required for the increased glycogen produced by mTORC1 activation. *A*: Western blots showing SREBP1 knockdown in TSC2 MEFs. See RESEARCH DESIGN AND METHODS for details. N.E., nuclear extracts; WCL, whole-cell lysate. Cells were transfected with lentiviral-mediated control shRNA or shRNAs targeting SREBP1 and selected for cells stably expressing shRNAs. Stable cells were lysed and subjected to Western blotting against indicated antibodies. *B*: Quantitative real-time PCR showing relative mRNA level of SREBP1 and PTG from cells in *A*. *C*: Glycogen content of cells in *A*. *D*: [^{14}C]glucose conversion into glycogen of cells in *A*. Data are mean ± SE (n = 3). *P < 0.05 by Student t test.

content. More importantly, these effects were blocked by overexpression of PTG mutants that are incompetent to bind to GS or GP, suggesting that PTG is crucial in the recruitment of GS and GP to glycogen particles (Supplementary Fig. 2*C*).

Homozygous Deletion of PTG Reduces Glycogen and Lipid Levels In Vivo

Our previous studies in PTG heterozygous KO mice suggested that PTG acts as a PP1 scaffolding protein and plays a vital role in glycogen metabolism (11). These mice had been maintained on a mixed background in which homozygous deletion of the PTG gene was lethal in the embryonic stage. Subsequent backcrosses of these mice into a C57BL/6J background produced viable homozygous PTG KO mice (Supplementary Fig. 3*A*). The genotyping of >200 female and male homozygous PTG KO pups derived from heterozygous breeding pairs coming from the first backcross accounted for only ~10% of the total births, a number significantly lower than the expected Mendelian inheritance ratio of 25% (Supplementary Fig. 3*B*). However, sequential backcross of the heterozygous PTG KO mice with C57BL/6J mice produced both female and male homozygous PTG KO mice born at the expected frequency (Supplementary Fig. 3*B*). Although the mechanism underlying the effect of genetic background on survival of PTG KO mice remains unknown, all the experiments described in the current study were performed on male PTG KO mice derived from heterozygous breeding pairs backcrossed 10 times with C57BL/6J mice, and littermates without PTG gene deletion (WT) were used as controls.

To study the role of PTG in glucose homeostasis in vivo, we fed PTG KO mice an HFD. No obvious differences in weight gain or food intake were observed between WT and KO mice fed either ND or HFD, demonstrating that the PTG KO mouse exhibits a normal growth rate and eating behavior (Supplementary Fig. 3*C* and *D*).

Both hepatic glycogen and triglyceride levels were greatly reduced in PTG KO mice fed an HFD for 12 weeks (Supplementary Fig. 3*E* and *F*). Consistent with the

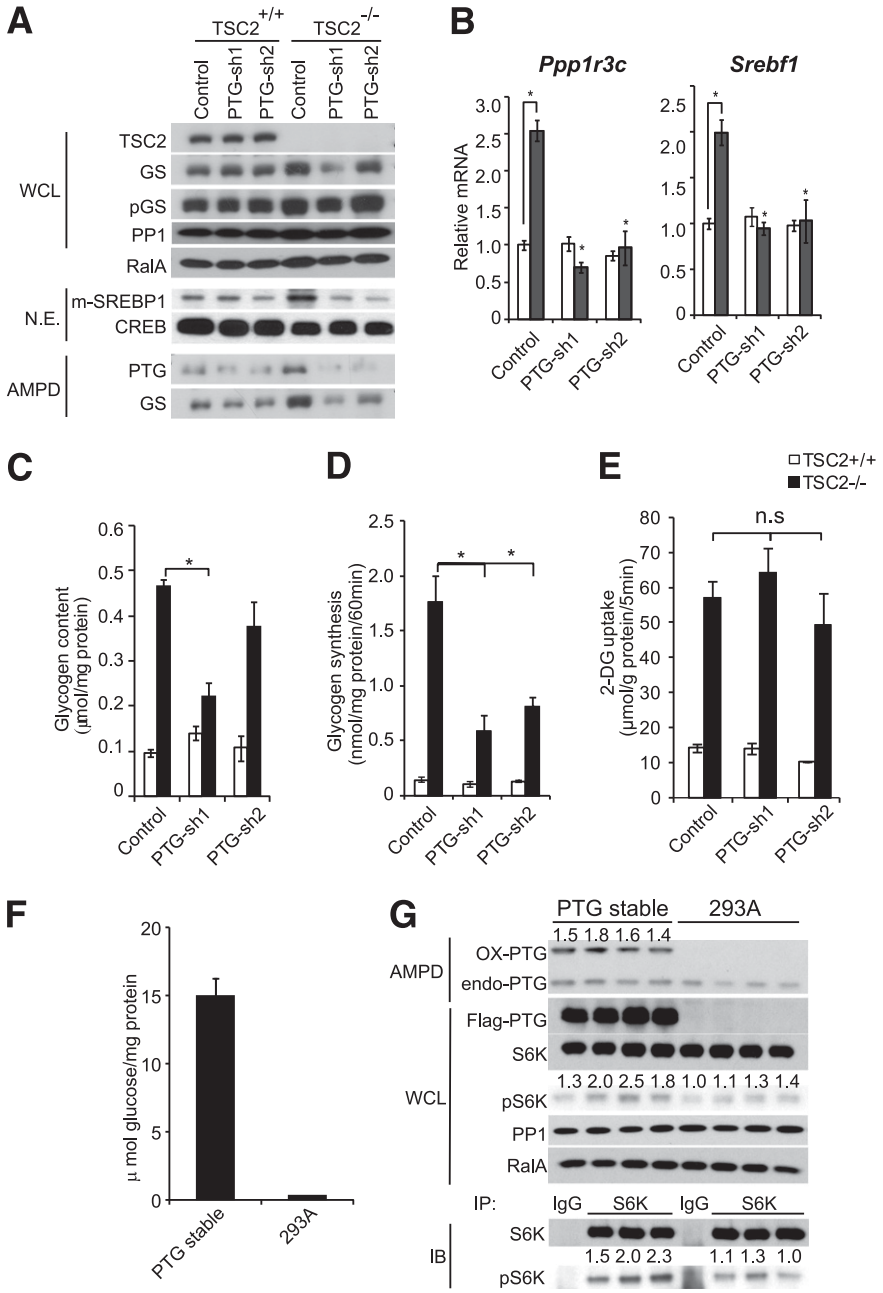

Figure 4—PTG levels control glycogen synthesis and contribute to feedback regulation of mTORC1 and SREBP1. *A*: Western blots showing PTG knockdown in TSC2 MEFs. Cells were transfected with lentiviral-mediated control shRNA or shRNAs targeting PTG and selected for cells stably expressing shRNAs. Stable cells were lysed and subjected to Western blotting against indicated antibodies. *B*: Quantitative real-time PCR showing relative mRNA level of PTG and SREBP1 from cells in *A*. *C*: Glycogen content of cells in *A*. *D*: [^{14}C]glucose conversion into glycogen of cells in *A*. *E*: 2-DG uptake of cells in *A*. *F*: Glycogen levels of HEK293A cells stably overexpressing Flag-tagged PTG. *G*: Representative Western blots showing activation of mTORC1 activity by overexpressing PTG. Numbers above blots indicate relative band intensity as quantified by NIH ImageJ software. Data are mean ± SE (n = 3 experiments). *$P < 0.05$ by Student t test. 2-DG, 2-deoxy-D-glucose; IB, immunoblotting; IP, immunoprecipitation; N.E., nuclear extracts; n.s., not significant by Student t test; WCL, whole-cell lysate.

increased hepatic glycogen levels observed in HFD WT mice, a twofold increase in PTG and SREBP1 mRNA was detected (Supplementary Fig. 3*G*). The mRNA levels of the glycogen-targeting subunit GL were also increased by about twofold under HFD conditions (Supplementary Fig. 3*G*). However, GTTs and ITTs were indistinguishable between PTG WT and KO mice fed either ND or HFD (Supplementary Fig. 3*H* and *I*). Of note, neither GS nor GP activity was changed in the liver lysates from KO mice (Supplementary Fig. 4), reinforcing the hypothesis that PTG is a crucial scaffold to recruit GS or GP to the glycogen particles. In this regard, it is possible that the

phosphorylation status or activity of nonglycogen-targeted GS or GP (i.e., GS or GP in whole-cell lysate) is largely irrelevant to glycogen accumulation.

We next explored glycogen synthesis more broadly by directly examining glucose conversion into glycogen in vitro in isolated primary hepatocytes (Fig. 5*A–C*) or in vivo during a hyperinsulinemic-euglycemic clamp study (Fig. 5*D* and *E*). In primary hepatocytes isolated from mice fed an ND, we observed a 60% reduction in [^{14}C] glucose incorporation into glycogen in PTG KO mice but no obvious difference in lipid or CO_2 incorporation, which is consistent with the mild reduction in triglycerides observed in PTG KO mice fed an ND. Both [^{3}H]glucose incorporation into glycogen and lipids were 40–50% reduced in PTG KO mice fed an HFD for 8–10 weeks, as measured in a hyperinsulinemic-euglycemic clamp study, suggesting that both glycogen and lipid synthesis in HFD-fed mice are reduced when PTG is depleted.

PTG Ablation Reduces Hepatic Steatosis After Long-term HFD

Because of the profound effects of PTG deletion on lipid accumulation in liver, we also studied mice fed an HFD for 24 weeks. Similar to what was observed with shorter-term HFD feeding, the 24-week HFD-induced elevation in glycogen was prevented in PTG KO mice (Fig. 6*A*). Triglyceride content was 40% decreased in livers from PTG KO mice fed an HFD compared with WT littermates, corresponding to decreased glycogen levels (Fig. 6*B*). Moreover, HFD-induced liver steatosis was significantly attenuated by PTG ablation, consistent with the marked reduction in triglycerides (Fig. 6*C*).

To further investigate alleviation of the hepatosteatotic phenotype, we measured the expression of key metabolic and inflammatory genes in the livers. PTG KO mice fed an HFD had lower expression of *Srebf1* and its downstream target gene fatty acid synthase (*Fasn*) (Fig. 6*D*). Gluconeogenic gene expression was modestly higher in HFD-fed mice and was not different with PTG ablation (Fig. 6*E*). However, glycolytic genes, such as pyruvate kinase isozymes R/L (*Pklr*) and glucokinase (*Gck*), which were more highly expressed in mice fed an HFD relative to those fed an ND, were expressed at lower levels in PTG KO mice (Fig. 6*E*). In addition, HFD-induced expression of several inflammatory genes and markers of macrophage infiltration, including F4/80 (*Emr1*), CD11C (*Itgax*), Rantes (*Ccl5*), and MCP-1 (*Ccl2*), were reduced in livers from PTG KO mice (Fig. 6*F*).

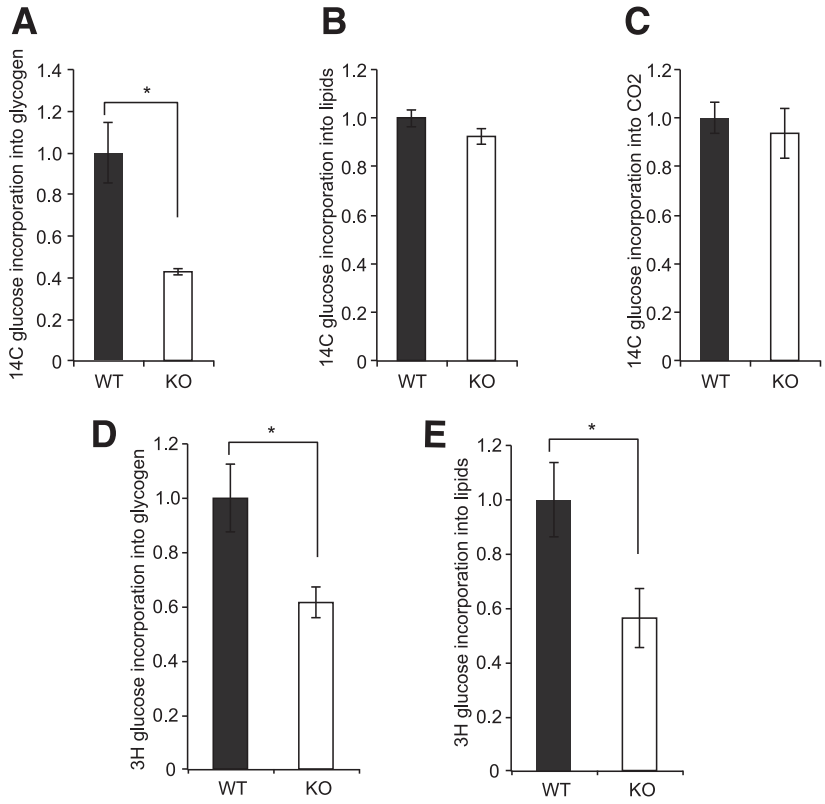

Figure 5—PTG ablation results in decreased glucose incorporation into glycogen and lipids. [^{14}C]glucose incorporation into glycogen (*A*), lipids (*B*), and CO_2 (*C*) in primary hepatocytes isolated from 6- to 8-week-old PTG WT or KO mice fed ND. Data are mean ± SE (n = 3 triplicate experiments). *Significant $P < 0.05$ by Student t test. [^{3}H]glucose incorporation into glycogen (*D*) and lipids (*E*) during a hyperinsulinemic-euglycemic clamp study using PTG WT or KO mice fed HFD for 8–10 weeks. Data are mean ± SE (n = 10–12 mice/group). *$P < 0.05$ by Student t test.

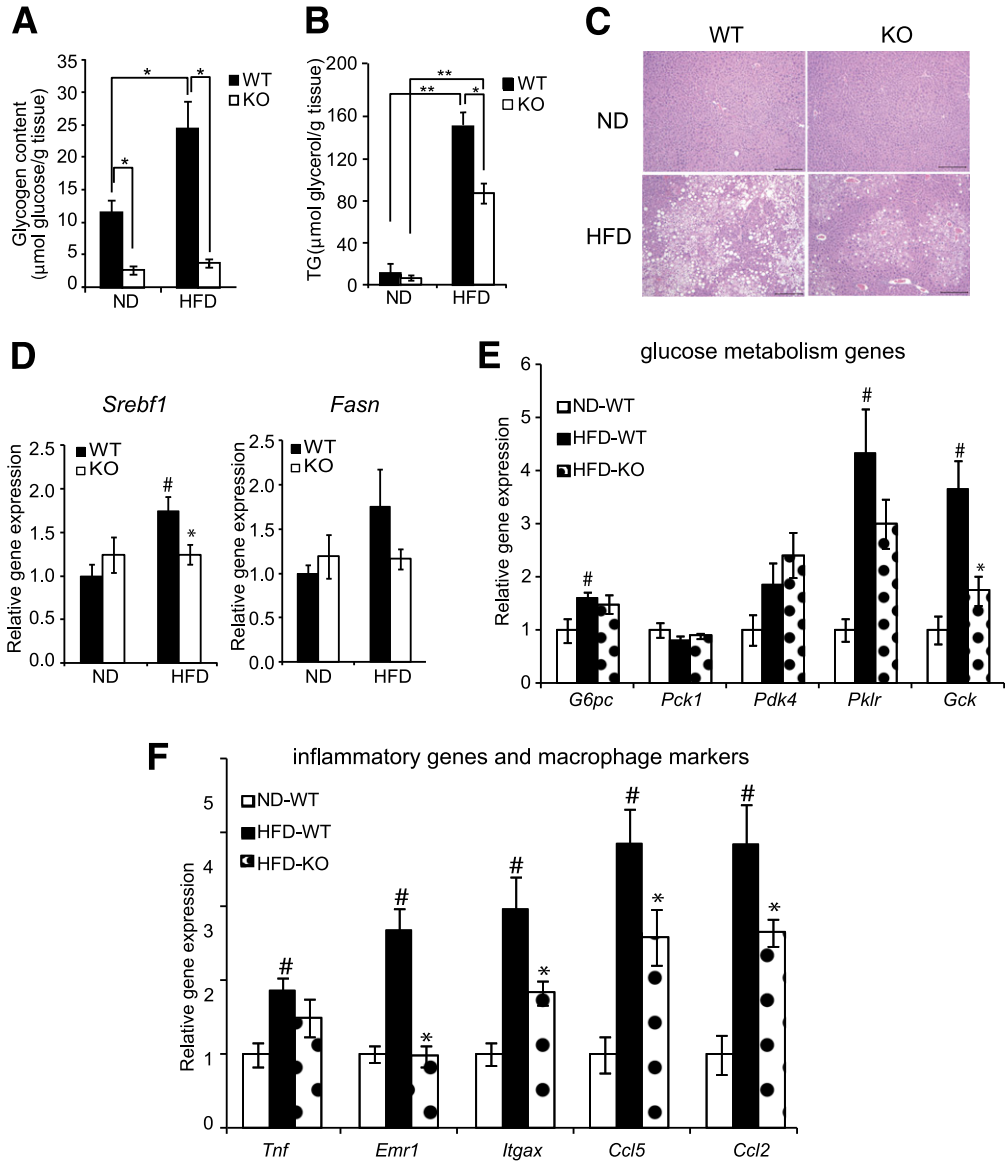

Figure 6—PTG ablation reduces hepatic steatosis in vivo after long-term HFD. *A* and *B*: Glycogen content and triglyceride levels, respectively, in the liver of WT and PTG KO mice fed HFD for 24 weeks and fasted overnight (n = 8–10 mice/group). *C*: Representative hematoxylin-eosin staining of liver sections of mice in *A* (scale bars = 200 μm). *D*: Quantitative real-time PCR showing relative mRNA level of SREBP1 and fatty acid synthase from mice in *A*. *E* and *F*: Quantitative real-time PCR showing relative mRNA level of glucose metabolism genes and inflammatory genes and macrophage markers, respectively, from mice in *A*. TG, triglyceride. *P < 0.05 HFD-KO versus HFD-WT; #P < 0.05 HFD-WT versus ND-WT.

PTG Ablation Improves Glucose Tolerance and Insulin Sensitivity After Long-term HFD

These changes in glycogen and lipid metabolism prompted us to investigate the role of PTG in the overall control of carbohydrate metabolism. After 24 weeks of HFD, both hyperglycemia and hyperinsulinemia were attenuated in PTG KO mice (Fig. 7*A*). We also performed oral GTTs, intraperitoneal ITTs, and PPTs. PTG ablation did not affect insulin sensitivity or glucose tolerance in ND-fed mice. However, PTG KO mice displayed much-improved glucose tolerance (Fig. 7*B*) as well as improved sensitivity to intraperitoneal injection of insulin (Fig. 7*C*) and pyruvate (Fig. 7*D*).

AMPD assays from liver lysates revealed that levels of glycogen-bound GS protein were increased by HFD consistent with the HFD-induced elevation in PTG protein levels (Fig. 7*E*). Moreover, the increase in glycogen-bound GS protein was suppressed in PTG KO mice, likely as a result of the lack of recruitment of GS to glycogen in the absence of PTG. These data demonstrate that the recruitment of GS to glycogen is elevated in HFD-fed mice due at least in part to increased PTG protein, causing increased hepatic glycogen content. Of note, both mTORC1 activity and SREBP1 levels were greatly attenuated in PTG KO mice, confirming in vivo the feedback

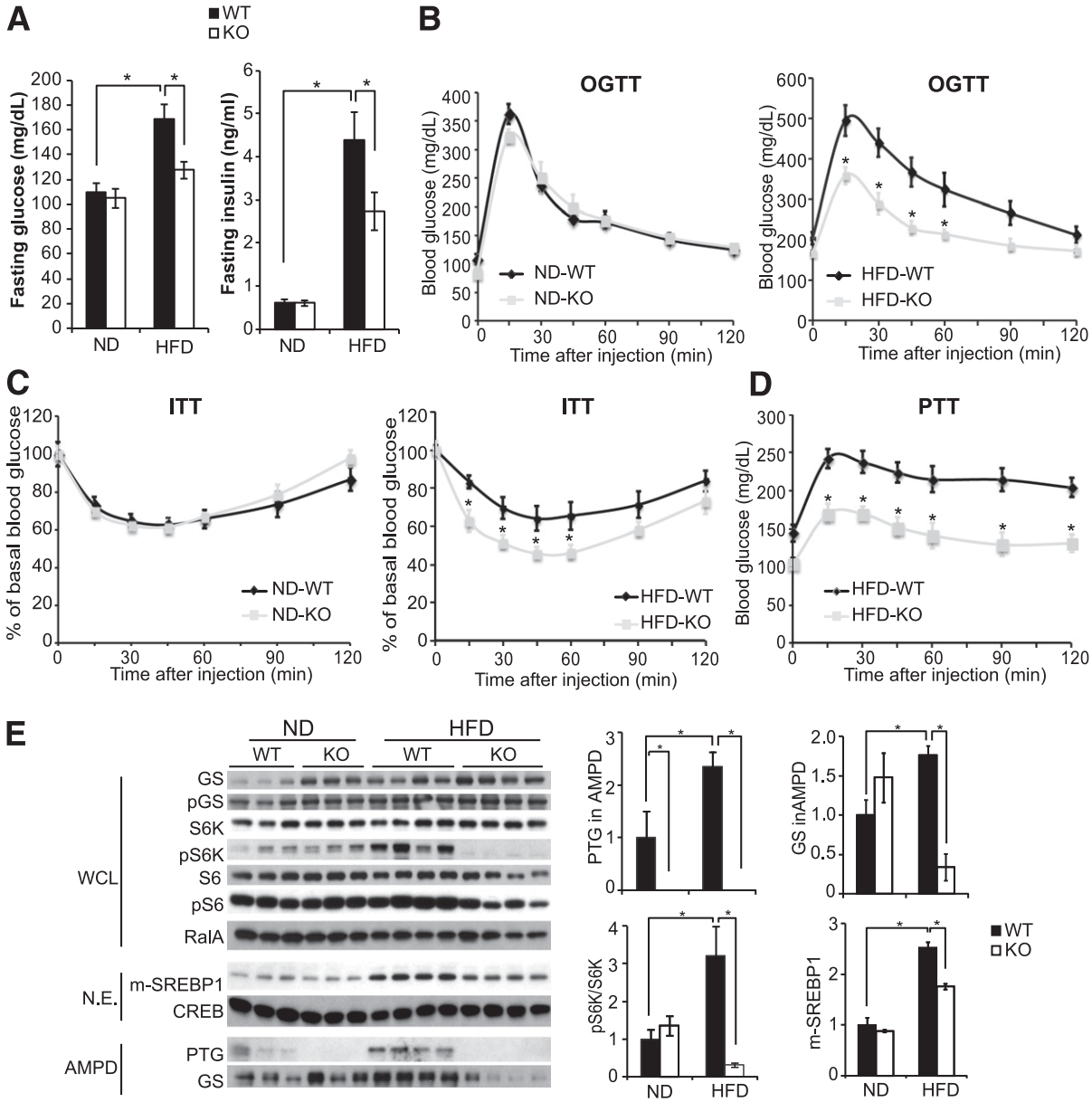

Figure 7—PTG ablation improves glucose tolerance and insulin sensitivity in vivo after long-term HFD. *A*: Fasting blood glucose and insulin levels of WT and PTG KO mice fed HFD for 24 weeks and fasted overnight. *B–D*: Oral GTTs, ITTs, and PTTs, respectively, of WT and PTG KO mice fed HFD for 24 weeks. *E*: Representative Western blot (*left*) and quantification (*right*) from the liver of mice in *A*. Data are mean ± SE (n = 8–10). *$P < 0.05$ by Student t test. N.E., nuclear extracts; OGTT, oral GTT; WCL, whole-cell lysate.

regulation of the mTORC1/SREBP1 pathway by PTG and glycogen.

Taken together, these results suggest that in short-term HFD-fed PTG KO mice, the reduction in hepatic glycogen likely contributes to lower glucose output while mildly reducing serum glucose and insulin levels. Over time, this modulation of metabolic activity also leads to dramatically improved insulin sensitivity in the KO mice, perhaps through reductions in mTORC1 activity known to negatively regulate insulin receptor signaling (21,22).

A PTG–SREBP1/mTORC1 Feedback Mechanism Regulates Lipogenesis

Although ablation of PTG did not have a major impact on systemic glucose tolerance and insulin sensitivity after short-term HFD, there were dramatic effects on hepatic lipid metabolism (Fig. 5*F*), which might reflect a crosstalk between pools of glycogen and upstream nutrient-sensing pathways. In an effort to determine the mechanism, we conducted quantitative real-time PCR for *Srebf1* and its target genes *Fasn, Ldlr*, and *Hmgcr*. We observed a trend toward decreases in the mRNA levels of these genes in the

PTG KO mice fed HFD, although these changes were not statistically significant (Fig. 8*A*).

To thoroughly examine the entire transcriptional landscape of PTG WT and KO livers, we performed unbiased RNA-seq and gene-set enrichment analysis. We found that sterol, steroid, cholesterol, and lipid biosynthetic/metabolic processes were differentially regulated by PTG ablation in HFD mice (Fig. 8*B*). More specifically, the transcript levels of *Srebf1* and its hepatic target genes, such as *Fasn*, *Ldlr*, *Mvk*, *Hmgcr*, were significantly reduced in the PTG KO mice (Fig. 8*C* and Supplementary Table 2), consistent with quantitative real-time PCR data. Collectively, these data reveal a novel crosstalk mechanism in which the mTORC1/SREBP pathway can sense elevated levels of glycogen and then initiate the transcriptional changes that increase lipid synthesis.

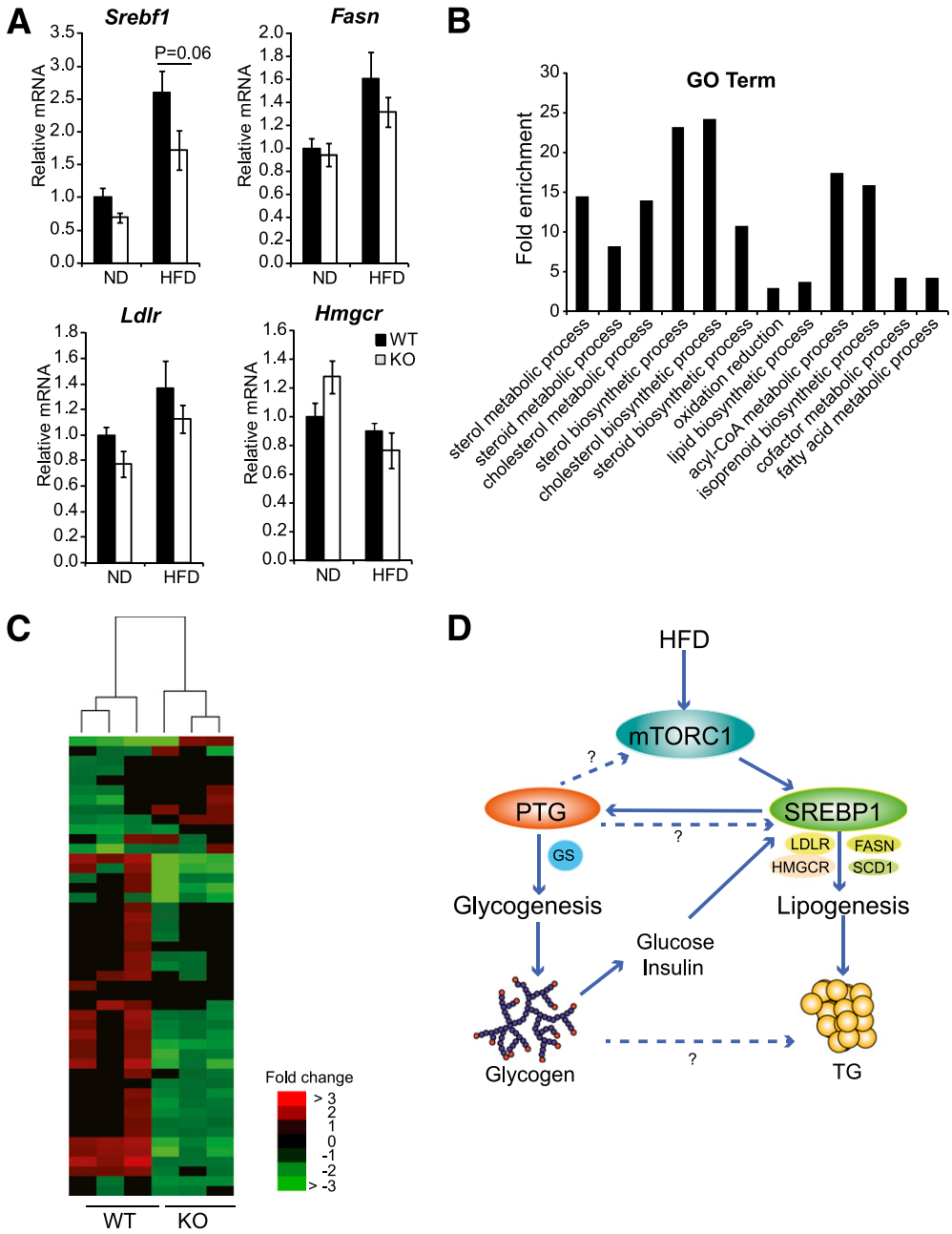

Figure 8—A PTG–SREBP1/mTORC1 feedback mechanism regulates lipogenesis. *A*: Quantitative real-time PCR showing relative mRNA level of SREBP1 and its target genes from the livers of mice fed HFD for 12 weeks and fasted overnight (n = 8–10 mice/group). *B*: Gene ontology term enrichment analysis of RNA-seq data from the livers of mice in *A*. *C*: Unbiased hierarchical clustering analysis of RNA-seq data from the livers of mice in *A*, showing downregulation of SREBP1 hepatic target genes in PTG KO mice fed HFD. Genes shown on the heat map are listed in Supplementary Table 2. *D*: A schematic model showing the feedback regulation of PTG and glycogen on mTORC1/SREBP1 and lipogenesis. GO, gene ontology; TG, triglyceride.

DISCUSSION

Despite its well-established role as the first choice for energy storage and mobilization, the coordination of glycogen metabolism with that of lipid synthesis and breakdown remains poorly understood, particularly in the liver. The present data reveal that upon reaching threshold levels during nutrient excess, glycogen may trigger increased expression of lipogenic genes, thus shifting energy storage from glycogen to lipid. This shift in the mode of energy storage may result from a positive feedback loop involving mTORC1 and its transcriptional factor target SREBP1.

The activation of GS by insulin requires the localization of PP1 to glycogen particles through glycogen-targeting subunits, which act as molecular scaffolds to unite PP1 with GS and GP for regulation (23). This study confirms the crucial role of PTG in controlling glycogen synthesis (4,5). PTG KO mice have markedly reduced glycogen levels in liver. Moreover, biochemical evaluation of GS localization in PTG KO mice demonstrates conclusively that PTG is essential to direct GS to glycogen particles in liver.

The present experiments also reveal the surprising finding that the regulation of glycogen synthesis by fasting/refeeding and HFD can be largely attributed to changes in the expression of PTG. The increase in glycogen levels found in the livers of HFD mice is mirrored by increased expression of PTG but attenuated in PTG KO mice. Both in vivo and in vitro studies revealed an important role for mTORC1 in PTG expression, consistent with findings by us and others that glycogen synthesis is sensitive to inhibition by rapamycin (24–26). We propose that mTORC1 may regulate glycogen metabolism through a transcriptional mTORC1/SREBP/PTG pathway, which in turn modifies the phosphorylation status of GS in the glycogen compartment (Fig. 8*D*). This idea is supported by studies in both embryonic fibroblasts and mice in which there was a clear causal relationship between mTORC1 function, SREBP, and PTG levels and glycogen accumulation. The regulation of SREBP processing by mTORC1 has been widely studied in the context of lipid homeostasis (27,28). The present data suggest that dietary modulations in mTORC1 activity may affect not only lipid storage but also carbohydrate storage through regulation of glycogen synthesis.

Also surprising was the effect of PTG ablation on glucose metabolism. PTG mice on the original mixed background were homozygous lethal, so we studied the heterozygous KOs and found that they have decreased hepatic glycogen levels and a worsened metabolic phenotype after ≥10 months of ND (11). However, we were surprised to find after several years that the homozygous PTG KO mice were viable by backcrossing heterozygotes against C57BL6/J mice. After short-term HFD, the new homozygous PTG KO mice showed reduced hepatic glucose output compared with WT littermates, but little effect on systemic insulin sensitivity, likely reflecting reduced glycogen that serves as a source of glucose. However, after longer-term HFD, PTG KO mice exhibited profoundly reduced fasting glucose and insulin levels along with improved glucose, pyruvate, and insulin tolerance, reflecting increased systemic insulin sensitivity. These were accompanied by changes in expression of genes involved in lipogenesis, glycolysis, inflammation, and macrophage infiltration. Thus, although GS is increased while GP is decreased by insulin action, and both enzymes have been considered as targets for the treatment of type 2 diabetes, reducing glycogen synthesis may paradoxically improve insulin resistance in obesity.

The effect of PTG deletion on hepatic steatosis was particularly intriguing. Because PTG does not interact with lipid-metabolizing enzymes, it is likely that this observation reflects crosstalk between pools of glycogen and upstream nutrient-sensing pathways. These ideas are consistent with observations from a study in which administration of a GP inhibitor resulted in a short-term reduction in blood glucose by preventing hepatic glycogen breakdown, but this effect was accompanied by steatosis after longer-term treatment due to increased lipid synthesis (29). Glycogen levels are increased in the livers of HFD mice under fasting conditions, whereas the mTORC1 pathway is constitutively elevated along with increased levels of PTG, suggesting that diet-induced activation of mTORC1 may increase glycogen stores in the fasted state by increasing the levels of PTG. This occurs even in the face of reduced insulin signaling in HFD and is similar to what is observed for obesity-induced hepatic triglyceride accumulation [reviewed in Brown and Goldstein [30]). Conversely, PTG KO mice, which have reduced levels of hepatic glycogen, have reduced hepatic lipids and reduced mTORC1/SREBP. Our transcriptional landscape analysis by RNA-seq revealed a significant down-regulation of SREBP1 and numerous target genes involved in lipogenesis. Although we cannot rule out other mechanisms explaining reduced hepatic lipid levels, such as reduced glucose and insulin levels, these transcriptional changes most likely underlie the alterations in lipid levels in PTG KO livers, which perhaps reflect an interesting feedback regulation of PTG on mTORC1/SREBP and lipogenesis to mediate crosstalk between pools of glycogen and lipids.

How might mTORC1 sense levels of glycogen? We propose a molecular sensor upstream of the mTORC1 complex, similar to what might be involved in the sensing of amino acids (31). One possible candidate is AMPK, a negative regulator of mTORC1 that is believed to be directly attenuated by the binding of glycogen to its β-subunit (32–34). Although we did not observe a decrease in AMPK or acetyl-CoA carboxylase phosphorylation in liver from PTG mice fed a short-term

HFD, there were reductions in muscle tissue (data not shown), suggesting that this enzyme may contribute to the overall regulation of mTORC1. However, the possibility remains that there are other glycogen sensors in the mTOR pathway. Future studies will focus on the regulation of this pathway by glycogen with the hope of developing new therapeutic targets for the treatment of insulin resistance and nonalcoholic fatty liver disease.

Acknowledgments. The authors thank the University of Michigan Vector Core and the Comprehensive Cancer Center Tissue Core for shRNA clones and histology service. The authors also thank Jay Horton for SREBP1 antibodies, David Kwiatkowski for the TSC2 KO fibroblasts, and Ken Inoki and the members of the Saltiel laboratory for helpful discussions.

Funding. This work was supported by a mentor-based postdoctoral fellowship from the American Diabetes Association to B.L. and grants from the National Institutes of Health (NIH) (DK-057978), the Leona M. and Harry B. Helmsley Charitable Trust, the Glenn Foundation for Medical Research, and the Ellison Medical Foundation to R.M.E. This work was also funded by NIH grants R24-DK-090962 to R.M.E. and A.R.S. and R01-DK-060591 to A.R.S.

Duality of Interest. No potential conflicts of interest relevant to this article were reported.

Author Contributions. B.L. contributed to the overall research plan, experiments, data analysis and interpretation, figure preparation, and writing of the manuscript. D.B. contributed to the experiments, data analysis and interpretation, and review and editing of the manuscript. Y.Y. and K.F. contributed to the experiments. A.C. and L.C. contributed to the experiments and data analysis and interpretation. Z.-X.M. and J.D.L. contributed to the primary hepatocyte experiment and data analysis and interpretation. M.D., R.T.Y., C.L., and R.M.E. contributed to RNA-seq and data analysis. A.R.S. contributed to the overall research plan, data interpretation, discussion, and review and editing of the manuscript. A.R.S. is the guarantor of this work and, as such, had full access to all the data in the study and takes responsibility for the integrity of the data and the accuracy of the data analysis.

Prior Presentation. Parts of this study were presented in abstract form at the 73rd Scientific Sessions of the American Diabetes Association, Chicago, IL, 21–25 June 2013.

References

1. Roach PJ, Depaoli-Roach AA, Hurley TD, Tagliabracci VS. Glycogen and its metabolism: some new developments and old themes. Biochem J 2012;441:763–787

2. Newgard CB, Brady MJ, O'Doherty RM, Saltiel AR. Organizing glucose disposal: emerging roles of the glycogen targeting subunits of protein phosphatase-1. Diabetes 2000;49:1967–1977

3. O'Doherty RM, Jensen PB, Anderson P, et al. Activation of direct and indirect pathways of glycogen synthesis by hepatic overexpression of protein targeting to glycogen. J Clin Invest 2000;105:479–488

4. Printen JA, Brady MJ, Saltiel AR. PTG, a protein phosphatase 1-binding protein with a role in glycogen metabolism. Science 1997;275:1475–1478

5. Brady MJ, Printen JA, Mastick CC, Saltiel AR. Role of protein targeting to glycogen (PTG) in the regulation of protein phosphatase-1 activity. J Biol Chem 1997;272:20198–20204

6. Yang R, Cao L, Gasa R, Brady MJ, Sherry AD, Newgard CB. Glycogen-targeting subunits and glucokinase differentially affect pathways of glycogen metabolism and their regulation in hepatocytes. J Biol Chem 2002;277:1514–1523

7. Gasa R, Jensen PB, Berman HK, Brady MJ, DePaoli-Roach AA, Newgard CB. Distinctive regulatory and metabolic properties of glycogen-targeting subunits of protein phosphatase-1 (PTG, GL, GM/RGl) expressed in hepatocytes. J Biol Chem 2000;275:26396–26403

8. Magistretti PJ, Allaman I. Glycogen: a Trojan horse for neurons. Nat Neurosci 2007;10:1341–1342

9. Allaman I, Pellerin L, Magistretti PJ. Protein targeting to glycogen mRNA expression is stimulated by noradrenaline in mouse cortical astrocytes. Glia 2000;30:382–391

10. Cheng A, Zhang M, Crosson SM, Bao ZQ, Saltiel AR. Regulation of the mouse protein targeting to glycogen (PTG) promoter by the FoxA2 forkhead protein and by 3′,5′-cyclic adenosine 5′-monophosphate in H4IIE hepatoma cells. Endocrinology 2006;147:3606–3612

11. Crosson SM, Khan A, Printen J, Pessin JE, Saltiel AR. PTG gene deletion causes impaired glycogen synthesis and developmental insulin resistance. J Clin Invest 2003;111:1423–1432

12. Pederson BA, Chen H, Schroeder JM, Shou W, DePaoli-Roach AA, Roach PJ. Abnormal cardiac development in the absence of heart glycogen. Mol Cell Biol 2004;24:7179–7187

13. Greenberg CC, Meredith KN, Yan L, Brady MJ. Protein targeting to glycogen overexpression results in the specific enhancement of glycogen storage in 3T3-L1 adipocytes. J Biol Chem 2003;278:30835–30842

14. Livak KJ, Schmittgen TD. Analysis of relative gene expression data using real-time quantitative PCR and the 2(-Delta Delta C(T)) method. Methods 2001;25:402–408

15. Horton JD, Bashmakov Y, Shimomura I, Shimano H. Regulation of sterol regulatory element binding proteins in livers of fasted and refed mice. Proc Natl Acad Sci U S A 1998;95:5987–5992

16. Trapnell C, Roberts A, Goff L, et al. Differential gene and transcript expression analysis of RNA-seq experiments with TopHat and Cufflinks. Nat Protoc 2012;7:562–578

17. Jiang T, Wang Z, Proctor G, et al. Diet-induced obesity in C57BL/6J mice causes increased renal lipid accumulation and glomerulosclerosis via a sterol regulatory element-binding protein-1c-dependent pathway. J Biol Chem 2005;280:32317–32325

18. Biddinger SB, Almind K, Miyazaki M, Kokkotou E, Ntambi JM, Kahn CR. Effects of diet and genetic background on sterol regulatory element-binding protein-1c, stearoyl-CoA desaturase 1, and the development of the metabolic syndrome. Diabetes 2005;54:1314–1323

19. Huang J, Manning BD. The TSC1-TSC2 complex: a molecular switchboard controlling cell growth. Biochem J 2008;412:179–190

20. Avruch J, Hara K, Lin Y, et al. Insulin and amino-acid regulation of mTOR signaling and kinase activity through the Rheb GTPase. Oncogene 2006;25:6361–6372

21. Shah OJ, Wang Z, Hunter T. Inappropriate activation of the TSC/Rheb/mTOR/S6K cassette induces IRS1/2 depletion, insulin resistance, and cell survival deficiencies. Curr Biol 2004;14:1650–1656

22. Um SH, Frigerio F, Watanabe M, et al. Absence of S6K1 protects against age- and diet-induced obesity while enhancing insulin sensitivity. Nature 2004;431:200–205

23. Brady MJ, Saltiel AR. The role of protein phosphatase-1 in insulin action. Recent Prog Horm Res 2001;56:157–173

24. Cross DA, Watt PW, Shaw M, et al. Insulin activates protein kinase B, inhibits glycogen synthase kinase-3 and activates glycogen synthase by rapamycin-insensitive pathways in skeletal muscle and adipose tissue. FEBS Lett 1997;406:211–215

25. Azpiazu I, Saltiel AR, DePaoli-Roach AA, Lawrence JC. Regulation of both glycogen synthase and PHAS-I by insulin in rat skeletal muscle involves mitogen-activated protein kinase-independent and rapamycin-sensitive pathways. J Biol Chem 1996;271:5033–5039

26. Shepherd PR, Navé BT, Siddle K. Insulin stimulation of glycogen synthesis and glycogen synthase activity is blocked by wortmannin and rapamycin in 3T3-L1 adipocytes: evidence for the involvement of phosphoinositide 3-kinase and p70 ribosomal protein-S6 kinase. Biochem J 1995;305(Pt. 1):25–28

27. Düvel K, Yecies JL, Menon S, et al. Activation of a metabolic gene regulatory network downstream of mTOR complex 1. Mol Cell 2010;39:171–183
28. Li S, Brown MS, Goldstein JL. Bifurcation of insulin signaling pathway in rat liver: mTORC1 required for stimulation of lipogenesis, but not inhibition of gluconeogenesis. Proc Natl Acad Sci U S A 2010;107:3441–3446
29. Floettmann E, Gregory L, Teague J, et al. Prolonged inhibition of glycogen phosphorylase in livers of Zucker diabetic fatty rats models human glycogen storage diseases. Toxicol Pathol 2010;38:393–401
30. Brown MS, Goldstein JL. Selective versus total insulin resistance: a pathogenic paradox. Cell Metab 2008;7:95–96
31. Zoncu R, Efeyan A, Sabatini DM. mTOR: from growth signal integration to cancer, diabetes and ageing. Nat Rev Mol Cell Biol 2011;12:21–35
32. McBride A, Ghilagaber S, Nikolaev A, Hardie DG. The glycogen-binding domain on the AMPK beta subunit allows the kinase to act as a glycogen sensor. Cell Metab 2009;9:23–34
33. Polekhina G, Gupta A, Michell BJ, et al. AMPK β subunit targets metabolic stress sensing to glycogen. Curr Biol 2003;13:867–871
34. Arad M, Benson DW, Perez-Atayde AR, et al. Constitutively active AMP kinase mutations cause glycogen storage disease mimicking hypertrophic cardiomyopathy. J Clin Invest 2002;109:357–362